SI information

SI Materials and Methods

Animals and animal care. Male adult C57BL/6 mice, aged 12 weeks (body weight 25ï 30g, Japan SLC, Inc., Hamamatsu, Japan) were used. sEH KO mice (body weight 26ï 32g) with targeted deletion of sEH gene (*Ephx2*) which is backcrossed to C57BL/6 background were used (61). Animals were housed under controlled temperatures and 12 hour light/dark cycles (lights on between 07:00ï 19:00 h), with ad libitum food (CE-2; CLEA Japan, Inc., Tokyo, Japan) and water. This study was carried out in strict accordance with the recommendations in the Guide for the Care and Use of Laboratory Animals of the National Institutes of Health, USA.

Materials. 1-Methyl-4-phenyl-1,2,3,6-tetrahydropyridine (MPTP: Tokyo Chemical Industry CO., LTD., Tokyo, Japan) was dissolved in saline. The sEH inhibitor TPPU, 1-trifluoromethoxyphenyl-3-(1-propionyl)piperidin-4-yl)urea, was synthesized as previously described (32). TPPU (0.3 ï 3.0 mg/kg) was dissolved in 10% polyethylene glycol 400 (PEG400: Wako Pure Chemical Co., Tokyo, Japan). Detailed information of antibodies used in this study was included in the Table S3. Other reagents were purchased commercially.

MPTP-induced mouse model of PD. First, mice were divided into four groups: (1): control group, (2-4): MPTP (10, 15, or 20 mg/kg x 3, 2-hr interval. 9:00, 11:00 and 13:00). Seven days after administration of MPTP, mice were deeply anesthetized with isoflurane and perfused transcardially with 10 ml of isotonic saline, followed by 40 ml of ice-cold 4% paraformaldehyde in 0.1 M phosphate buffer (pH 7.4). Brains were removed from the skulls and postfixed overnight at 4°C, and brain was used for immunohistochemistry of dopamine transporter (DAT) and tyrosine hydrogenase (TH).

Second, mice were randomly divided into six groups: (1): control group, (2): MPTP groups, (3) TPPU group. MPTP (10 mg/kg x 3, 2-hr interval. 9:00, 11:00 and 13:00) or saline (10 ml/kg x 3, 2-hr interval) was injected into mice. Vehicle (10 ml/kg) or TPPU (0.3, 1.0, or 3 mg/kg. 19:00) was administered orally 6 hours after the final administration of saline or MPTP. Subsequently, vehicle or TPPU (3.0 mg/kg) were injected orally twice daily (9:00 and 19:00) for additional 6 days (days 2 ï 7). Mice were sacrificed on day 8, and striatum from mouse brain was collected. Brain samples

were stored at -80°C before the use of high performance liquid chromatography (HPLC).

Third, mice were divided into four groups: (1): control group, (2-4): MPTP (10 mg/kg x 3, 2-hr interval). MPTP (10 mg/kg x 3, 2-hr interval. 9:00, 11:00 and 13:00) or saline (10 ml/kg x 3, 2-hr interval) was injected i.p. into mice. Vehicle (10 ml/kg) or TPPU (3 mg/kg) were administered orally 6 hours after the final administration of saline or MPTP. Subsequently, vehicle or TPPU (3.0 mg/kg) were injected orally twice day (9:00 and 19:00) for additional 6 days (days 2 ï 7). On day 8, mice were deeply anesthetized with isoflurane and perfused transcardially with 10 ml of isotonic saline, followed by 40 ml of ice-cold 4% paraformaldehyde in 0.1 M phosphate buffer (pH 7.4). Brains were removed from the skulls and postfixed overnight at 4°C, and brain was used for immunohistochemistry.

Fourth, wild mice and sEH KO mice were divided into two groups, respectively. Subsequently, these two groups were divided into control group and MPTP (10 mg/kg x 3, 2-hr interval. 9:00, 11:00 and 13:00). On day 8, mice were deeply anesthetized with isoflurane and perfused transcardially with 10 ml of isotonic saline, followed by 40 ml of ice-cold 4% paraformaldehyde in 0.1 M phosphate buffer (pH 7.4). Brains were removed from the skulls and postfixed overnight at 4°C, and brain was used for immunohistochemistry.

Measurement of DA, DOPAC, and HVA in mouse striatum by HPLC. Tissue levels of DA and its metabolites (DOPAC, HVA) were measured as previously reported (62,63). Tissue samples (striatum) were homogenized in 0.2 M perchloric acid ($HClO_4$) containing 100 μM disodium EDTA and 100 ng/ml isoproterenol (internal standard), and were then centrifuged at 20,000×g for 15 min at 4°C. The supernatants were filtered through a 0.45-μm pore membrane (Millex-LH, 4 mm; Millipore, Tokyo, Japan) and were analyzed for 5-HT, 5-HIAA, DA, and DOPAC by HPLC coupled with electrochemical detection. The HPLC system consisted of a liquid chromatograph pump (EP-300, Eicom, Kyoto, Japan), a degasser (DG-300, Eicom, Kyoto, Japan), a reversed phase column (Eicompak SC-5ODS 150×3.0 mm; Eicom, Kyoto, Japan), an ECD-300 electrochemical detector (Eicom, Kyoto, Japan), and a data processor (EPC-300, Eicom, Kyoto, Japan). The mobile phase was 0.1 M acetate-citric acid buffer (pH 3.5)

containing 16% methanol, 5 mg/l disodium EDTA and 190 mg/l sodium octyl sulfate.

Immunohistochemistry of DAT, TH and OX42 in mouse brains.

Immunohistochemistry of DAT and TH was performed as reported previously (62-64). The mouse brain sections (Bregma 0.86ī 1.54mm) were identified according to stereotaxic coordinates in Franklin and PaxinosôMouse Brain (65). Free-floating sections were treated with 0.3% H_2O_2 in 0.05M Tris-HCl saline (TBS) for 30 min and blocked in TBS containing 0.2% Triton X-100 (TBST) and 1.5% normal serum for 1 hour, at room temperature. Samples were then incubated for 36 hours at 4°C, with rat anti-DAT antibody or with rabbit TH antibody. The sections were washed three in TBST, and processed according to the avidin-biotin-peroxidase method (Vectastain Elite ABC, Vector Laboratories, Inc., Burlingame, CA, USA). Sections were then incubated for 5 minutes in a solution of 0.15 mg/ml diaminobenzidine, containing 0.01% H_2O_2. The sections were mounted on gelatinized slides, dehydrated, cleared, and coverslipped under Permount® (Fisher Scientific, Fair Lawn, NJ, USA).

For immunofluorescence detection of TH and OX42, the mouse brain section (Bregma 0.86ī 1.54mm and -2.92 ī -3.88 mm) were identified according to stereotaxic coordinates in Franklin and PaxinosôMouse Brain (65). The brain sections were blocked in TBS containing 0.2% Triton X (TBST) and 1.5% normal serum for 1 hour at room temperature. Then, sections were incubated overnight at 4°C, with rabbit TH antibody or rat OX42 antibody. Next day, sections were washed three times in TBST, and incubated in fluorochrome-conjugated secondary antibody diluted in antibody dilution for 2hours at room temperature in the dark. After wash three times with TBST, the sections were coverslipped under Prolong® Gold Antifade Reagent (Cell Signaling Technology, USA).

The staining intensity of DAT or TH immunoreactivity in the anterior regions (0.25 mm^2) of the striatum, and the number of TH-positive cells in SNc and OX42-postive cells in striatum (0.06mm^2) were imaged and analyzed using Keyence BZ-9000 Generation microscope (Keyence Co., Ltd, Osaka, Japan) and ImageJ software package.

Viral vector preparation and injection. The transfer plasmid (pAAV-CAGGS-Ephx2-P2A-EmGFP) was constructed by Invitrogen. The viral vectors

were prepared as described previously (66). Briefly, the AAV vectors were packaged using the AAV Helper Free Expression System (Cell Biolabs, Inc., San Diego, CA). The packaging plasmids (pAAV-DJ and pHelper) and transfer plasmid (pAAV-CAGGS-Ephx2-P2A-EmGFP or pAAV-CAGGS-EGFP) were transfected into HEK293T cells using the calcium phosphate method. After 48h incubation, AAV vector particles were obtained and purified by serial ultracentrifugation with cesium chloride. The purified particles were dialyzed with PBS, and then concentrated by ultrafiltration using an Amicon 10k MWCO filter (Merck Millipore, Darmstadet, Germany). The copy number of the viral genome (vg) was determined by the TaqMan Universal Master Mix II (Applied Biosystems, Foster City, CA). Real-time quantitative PCR was performed in duplicate samples using the StepOne real-time PCR system as follows: 95℃ for 10min; 40 cycles of (95℃, 15s and 60℃, 1min).

To induce gene expression in the striatum, AAV DJ-CAGGS-Ephx2-P2A-EmGFP or AAV DJ-CAGGS-EGFP vectors (1.0×10^{12} vg/ml) were stereotaxically injected into the striatum of C57BL/6 male mice at 9 weeks old by microinjection tube connected to a microinfusion pump (0.5 ε l/site, 0.1 ε l/min). The anteroposterior, mediolateral, and dorsoventral coordinates relative to Bregma were as follows: +1.1 mm, ±1.0 mm and ī 3.0 mm (65).

Western blot analysis of mouse brain samples. Western blot analysis was performed as reported previously (25,67). Mice were killed by cervical dislocation and brains were rapidly removed from the skull, and the striatum of mice were dissected on ice. The tissue samples were homogenized in Leammli lysis buffer. 50 μg of protein were measured using the DC protein assay kit (Bio-Rad), and incubated for 5 min at 95 , with an equal volume of 125 mM Tris-HCl, pH6.8, 20% glycerol, 0.1% bromophenol blue, 10% ϐ-mercaptoethanol, 4% sodium dodecyl sulfate, and subjected to sodium dodecyl sulfate polyacrylamide gel electrophoresis, using 7.5% or AnyKD mini-gels (Mini-PROTEAN® TGXÊ Precast Gel; Bio-Rad, CA, USA). Proteins were transferred onto polyvinylidenedifluoride (PVDF) membranes using a Trans Blot Mini Cell (Bio-Rad). For immunodetection, the blots were blocked with 2% BSA in TBST (TBS + 0.1% Tween-20) for 1 h at room temperature (RT), and kept with primary antibodies overnight at 4°C. The primary antibodies were used (Table S3). The next day, blots were washed three times in TBST and incubated with horseradish peroxidase conjugated

anti-rabbit or anti-mouse antibody 1 hour, at RT. After final three washes with TBST, bands were detected using enhanced chemiluminescence (ECL) plus the Western Blotting Detection system (GE Healthcare Bioscience). Images were captured with a ChemDoc imaging system (Bio-Rad), and the immunoreactive bands were analysis by Image Lab software.

Western blot analysis of postmortem brain samples. The postmortem brain samples from DLB patients (n = 10, age: 86.7 ± 2.28 years old (range: 72 ï 93), 9 male and 1 female) and age-matched controls (n = 10, age 79.1 ± 3.19 years old (range: 62 ï 94), 8 male and 2 female)) were collected at Tokyo Metropolitan Geriatric Hospital and Institute of Gerontology (Tokyo, Japan). Brain samples were selected using the Brain Bank for Aging Research (BBAR) Lewy bodies rating system (68). Stages III to V correspond to the Lewy body diseases cases of PD, PD with dementia, and DLB (including DLB with Alzheimerôs disease)(69,70). Western blot analysis of DAT, TH, Ŭ-synuclein and phosphorylated Ŭ-synuclein in the striatum was performed as described above.

Oxylipin profiling. Mice were divided into control group and MPTP (10 mg/kg x 3, 2-hr interval. 9:00, 11:00 and 13:00). On day 8, mice were deeply anesthetized with isoflurane and brains were removed from the skulls. Striatum was dissected from brain, and the samples were stored at -80 before assay. Measurement of eicosanoids was performed using the previous method (71).

Human iPS cells. The control human iPSC lines 201B7 (72) and familial PD (PARK2) lines PB20 (34) were cultured on mitomycin C-treated SNL murine fibroblast feeder cells in iPSC medium, according to the previous report (72).

Total RNA isolated from induced Neuron from iPSC using RNeasy mini Kit (QIAGEN), according to the manufacturerôs instructions. cDNA was generated from 0.5 µg of total RNA with SuperScript® reverse transcriptase (Invitrogen) and random Hexamers (Invitrogen). qPCR analysis was performed with SYBR premix Ex Taq (TaKaRa) on QuantStudio 7 Flex (Applied Biosystems). Values were normalized to ß-actin and were analyzed by comparative (qpqpCt) methods. The primer sequences were as follows: human sEH forward 5ô- ACTTCGTGCTCGTTCCTCAG-3ô, Human sEH reverse 5ô-AGTGCCCACAGTCCTCAATG-3ô, Human ß-actin forward

5ô-TGAAGTGTGACGTGGACATC-3ô, Human ß-actin reverse 5ô-GGAGGAGCAATGATCTTGAT-3ô.

For the differentiation of midbrain dopaminergic (mDA) neurons, we used a previously reported method (73-75), with slight modifications. Briefly, the iPSCs were cultured in iPSC medium supplemented with 3 µM SB431542 (Tocris), 3 µM Dorsomorphin (Sigma), and 3 µM CHIR99021 (Stemgent) for 5 days. For neurosphere formation, iPSC colonies were dissociated into single cells by TrypLE Select (Life technologies) and cultured in medium hormone mix (MHM) medium (KOHJIN BIO) supplemented with B27 (Life technologies), 20 ng/ml basic fibroblast growth factor (bFGF: Pepro Tech), 2 µM SB431542 (Tocris), 5 µM Y27632 (Wako) in 4% O_2. Defining the day on which neurosphere culture was started as day 0, on day 3, 3 µM CHIR99021, and 2 µM Purmorphamine (Millipore) were added to culture medium. For terminal differentiation, on day 14, neurospheres were dissociated and seeded on poly-L-ornithine (Sigma) and Fibronectin (Corning)-coated 96 well culture plates in MHM supplemented with B27, 20 ng/ml brain-derived neurotrophic factor (BDNF; Biolegend), glial cell-derived neurotrophic factor (GDNF; Pepro Tech), 200 µM ascorbic acid (Sigma), 0.5 mM dibutyryl-cAMP (Nakalai Tesque), 1 ng/ml transforming growth factor ß (TGF-ß: Biolegend) and 10 µM DAPT (Sigma), and cultured for 17 days before analysis. Apoptosis was quantified and evaluated by the intensity of Cleaved Caspase-3 staining using IN Cell Analyzer 2200 (GE Healthcare). The mDA neurons were incubated with 10 µM TPPU or 0.1% DMSO as controls, for 10 days. After 10 days, mDA neuron were fixed with 4% paraformaldehyde (PFA) in PBS for 30 min at room temperature. Nonspecific proteins were blocked with 5% FBS and 0.3% Triton X-100 in PBS, and stained with the following primary antibodies; ß3-tubulin, TH, cleaved Caspase-3. The cells were then rinsed with incubated with species specific Alexa Fluor 488-, Alexa Fluor 555-, or Alexa Fluor 647-conjugated secondary antibodies, and Hoechst 33258 (1:5000; Sigma) for 1h at room temperature. The well for each experimental condition was duplicated. Fixed and Stained plates mDA neuron were imaged by IN Cell Analyzer 2200 (GE Healthcare), and 25 fields were collected from each well using 20x objective. The images were analyzed by IN Cell Developer Toolbox v1.9 (GE Healthcare), and identified nuclei with Hoechst, neuronal cell body

with ß3-tubulin, dopaminergic neuron with TH, and apoptosis with Cleaved Caspase-3. By setting the areas of ß3-tubulin and TH-positive cells, the intensity of Cleaved Caspase-3 in dopaminergic neurons was analyzed.

Statistical analysis. The data show as the mean ± standard error of the mean (S.E.M.). Analysis was performed using GraphPad Prism (La Jolla, CA). Comparisons between groups were performed using the one-way analysis of variance (ANOVA) or two-way ANOVA, followed by Fisherôs LSD test. Comparisons between two groups were performed using Student t-test. The P-values of less than 0.05 were considered statistically significant.

References

61. Sinai CJ, et al (2000) Targeted disruption of soluble epoxide hydrolase reveals a role in blood pressure regulation. *J Biol Chem* 275:40504ï 40510.
62. Koike K, et al (2005) The immunophilin ligand FK506 protects against methamphetamine-induced dopaminergic neurotoxicity in mouse striatum. *Neuropharmacology* 48:391ï 397.
63. Zhang L, et al (2006) Protective effects of minocycline on behavioral changes and neurotoxicity in mice after administration of methamphetamine. Prog Neuropsychopharmacol Biol Psychiatry 30:1381ï 1393.
64. Ren Q, Zhang JC, Ma M, Fujita Y, Wu J, Hashimoto K (2014) 7,8-Dihydroxyflavone, a TrkB agonist, attenuates behavioral abnormalities and neurotoxicity in mice after administration of methamphetamine. *Psychopharmacology (Berl)* 231:159ï 166.
65. Paxinos G, Franklin K (2002) Paxinos and Franklinôs the Mouse Brain in Stereotaxic Coordinates, 4th Edition. Academic Press.
66. Kobayashi K, et al (2016) Survival of corticostriatal neurons by Rho/Rho-kinase signaling pathway. *Neurosci Lett* 630:45ï 52.
67. Ren Q, et al (2015) BDNF-TrkB signaling in the nucleus accumbens shell of mice has key role in methamphetamine withdrawal symptoms. *Transl Psychiatry* 5:e666.
68. Saito Y, et al (2003) Accumulation of phosphorylated alpha-synuclein in aging human brain. *J Neuropathol Exp Neurol* 62:644ï 654.
69. Morimoto S, et al (2017) Homovanillic acid and 5-hydroxyindole acetic acid as biomarkers for dementia with Lewy bodies and coincident Alzheimer's disease: An autopsy-confirmed study. *PLOS One* 12:e0171524.

70. Saito Y, et al (2004) Lewy body-related α-synucleinopathy in aging. *J Neuropathol Exp Neurol* 63:742ï 749.
71. Yang J, Schmelzer K, Georgi K, Hammock BD (2009) Quantitative profiling method for oxylipin metabolome by liquid chromatography electrospray ionization tandem mass spectrometry. *Anal Chem* 81:8085ï 8093.
72. Takahashi K, et al (2007) Induction of pluripotent stem cells from adult human fibroblasts by defined factors. *Cell* 131:861ï 872.
73. Imaizumi K, et al (2015) Controlling the regional identity of hPSC-derived neurons to uncover neuronal subtype specificity of neurological disease phenotypes. *Stem Cell Reports* 5:1010ï 1022
74. Matsumoto T, (2016) Functional neurons generated from T cell-derived induced pluripotent stem cells for neurological disease modeling. *Stem Cell Reports* 6:422ï 435.
75. Fujimori K, Matsumoto T, Kisa F, Hattori N, Okano H, and Akamatsu W (2017) Escape from pluripotency via inhibition of TGF-ß/BMP and activation of Wnt signaling accelerates differentiation and aging in hPSC progeny cells. *Stem Cell Reports* 9:1675ï 1691.

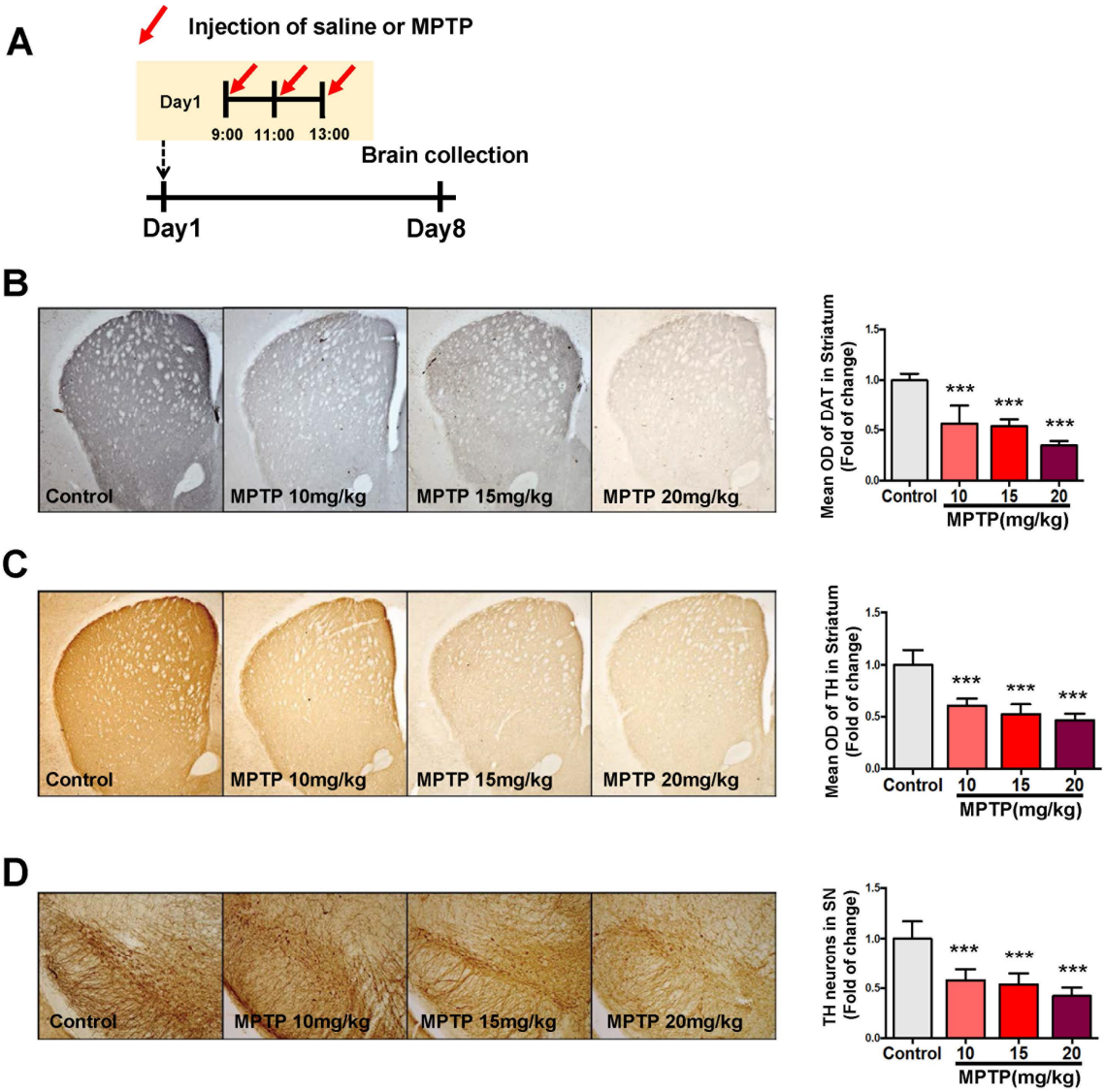

Figure S1. Effects of MPTP-induced neurotoxicity in the mouse brain. (A): Schedule of treatment and brain collection. (B-D): MPTP (10, 15, or 20 mg/kg x 3, 2-hr interval, IP, 9:00, 11:00, and 13:00) or saline was administered into mice. On day 8, mice were perfused for immunohistochemistry of DAT and TH. (B): Typical immunohistochemistry of DAT in the striatum. One-way ANOVA revealed the results ($F_{3,17}$ = 30.29, P < 0.001). (C): Typical immunohistochemistry of TH in the striatum. One-way ANOVA revealed the results ($F_{3,17}$ = 31.63, P < 0.001). (D): Typical immunohistochemistry of TH in the SN. One-way ANOVA revealed the results ($F_{3,17}$ = 21.07, P < 0.001). Data are shown as mean ± S.E.M. (n = 5 or 6). ***P < 0.001 compared to control group.

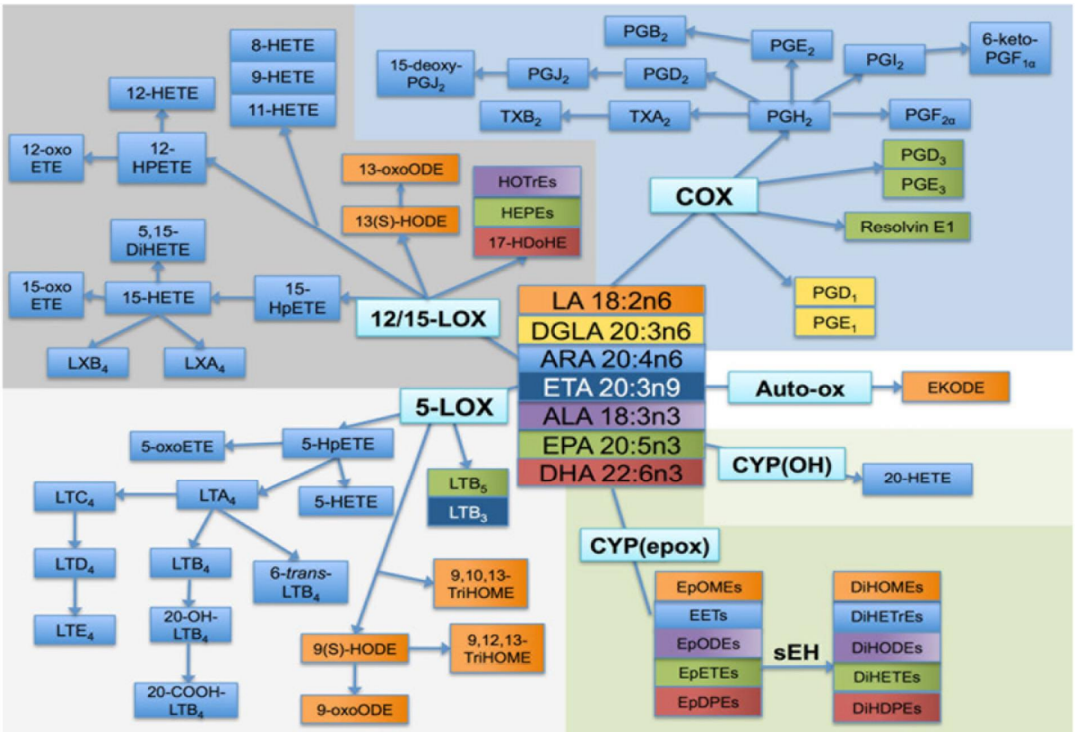

Figure S2. Eicosanoids measured in the striatum from control and MPTP-treated mice

Table S1. Detailed data of statistical analyses.

	Graph	Statistical test	Power	Factor effect		Interaction effect
Fig.1 B	DA	One-way ANOVA	n=7~8	$F_{5,41}$ = 19.01, P < 0.001		
Fig.1 C	DOPAC	One-way ANOVA	n=7~8	$F_{5,41}$ =13.94, P < 0.001		
Fig.1 D	HVA	One-way ANOVA	n=7~8	$F_{5,41}$ = 18.74, P < 0.001		
Fig.1 G	DAT	Two-way ANOVA	n=6	MPTP: $F_{1,20}$ = 12.65, P = 0.002	TPPU: $F_{1,20}$ = 2.846, P = 0.107	$F_{1,20}$ = 11.18, P = 0.003
Fig.1 H	TH	Two-way ANOVA	n=6	MPTP: $F_{1,20}$ = 26.57, P < 0.001	TPPU: $F_{1,20}$ = 29.76, P < 0.001	$F_{1,20}$ = 13.12, P = 0.0017
Fig.1 J	TH	Two-way ANOVA	n=6	MPTP: $F_{1,20}$ = 17.46, P = 0.0005	TPPU: $F_{1,20}$ = 4.274, P = 0.052	$F_{1,20}$ = 14.92, P = 0.001
Fig.2 B	DA	Two-way ANOVA	n=8	MPTP: $F_{1,28}$ = 14.52, P = 0.0007	KO: $F_{1,28}$ = 6.096, P = 0.0199	$F_{1,28}$ = 4.837, P = 0.0363
Fig.2 C	DOPAC	Two-way ANOVA	n=8	MPTP: $F_{1,28}$ = 7.822, P = 0.0092	KO: $F_{1,28}$ = 4.189, P = 0.0502	$F_{1,28}$ = 4.980, P = 0.0338
Fig.2 D	HVA	Two-way ANOVA	n=8	MPTP: $F_{1,28}$ = 3.753, P = 0.0637	KO: $F_{1,28}$ = 7.985, P = 0.0089	$F_{1,28}$ = 5.174, P = 0.0314
Fig.2 G	DAT	Two-way ANOVA	n=8	MPTP: $F_{1,28}$ = 6.692, P = 0.0154	KO: $F_{1,28}$ = 19.47, P = 0.0001	$F_{1,28}$ = 4.788, P = 0.0375
Fig.2 H	TH	Two-way ANOVA	n=8	MPTP: $F_{1,28}$ = 37.38, P < 0.0001	KO: $F_{1,28}$ = 2.322, P = 0.1387	$F_{1,28}$ = 15.57, P = 0.0005
Fig.2 J	TH	Two-way ANOVA	n=8	MPTP: $F_{1,28}$ = 22.69, P < 0.0001	KO: $F_{1,28}$ = 18.23, P = 0.0002	$F_{1,28}$ = 13.41, P = 0.0010
Fig.2 L	OX42	Two-way ANOVA	n=4	MPTP: $F_{1,12}$ = 89.54, P < 0.0001	KO: $F_{1,12}$ = 17.15, P = 0.0014	$F_{1,12}$ = 28.71, P = 0.0002
Fig.2 O	DAT	Two-way ANOVA	n=6	MPTP: $F_{1,20}$ = 17.80, P = 0.0004	KO: $F_{1,20}$ = 4.890, P = 0.0388	$F_{1,20}$ = 9.378, P = 0.0061
Fig.3 A	p-PERK/PERK	Two-way ANOVA	n=7	MPTP: $F_{1,24}$ = 3.784, P = 0.0636	TPPU: $F_{1,24}$ =0.8376, P = 0.3692	$F_{1,24}$ = 4.600, P = 0.0423
	p-eIF2α/eIF2α	Two-way ANOVA	n=7	MPTP: $F_{1,24}$ = 4.483, P = 0.0448	TPPU: $F_{1,24}$ = 5.748, P = 0.0246	$F_{1,24}$ = 18.67, P = 0.0002
	Bip	Two-way ANOVA	n=7	MPTP: $F_{1,24}$ = 13.83, P = 0.0011	TPPU: $F_{1,24}$ = 4.264, P = 0.0499	$F_{1,24}$ = 6.871, P = 0.0150
	p-IRE1/IRE1	Two-way ANOVA	n=7	MPTP: $F_{1,24}$ = 8.738, P = 0.0069	TPPU: $F_{1,24}$ = 1.472, P = 0.2369	$F_{1,24}$ = 12.80, P = 0.0015
	sXBP-1	Two-way ANOVA	n=7	MPTP: $F_{1,24}$ = 11.37, P = 0.0025	TPPU: $F_{1,24}$ = 6.163, P = 0.0204	$F_{1,24}$ = 5.745, P = 0.0247
	p-JNK/JNK	Two-way ANOVA	n=7	MPTP: $F_{1,24}$ = 3.597, P = 0.070	TPPU: $F_{1,24}$ = 6.319, P = 0.0191	$F_{1,24}$ = 4.528, P = 0.0438
	ATF6	Two-way ANOVA	n=7	MPTP: $F_{1,24}$ = 23.36, P < 0.0001	TPPU: $F_{1,24}$ = 1.219, P = 0.2804	$F_{1,24}$ = 9.943, P = 0.0043
	cATF6	Two-way ANOVA	n=7	MPTP: $F_{1,24}$ = 16.72, P = 0.0004	TPPU: $F_{1,24}$ = 1.042, P = 0.3175	$F_{1,24}$ = 6.880, P = 0.0149
	p-p38/p38	Two-way ANOVA	n=7	MPTP: $F_{1,24}$ = 0.7386, P = 0.3986	TPPU: $F_{1,24}$ = 7.842, P = 0.010	$F_{1,24}$ = 60.53, P < 0.0001
Fig.3 B	p-PERK/PERK	Two-way ANOVA	n=6~7	MPTP: $F_{1,21}$ = 11.70, P = 0.0026	KO: $F_{1,21}$ = 24.60, P < 0.0001	$F_{1,21}$ = 4.472, P = 0.0466
	p-eIF2α/eIF2α	Two-way ANOVA	n=6~7	MPTP: $F_{1,21}$ = 1.412, P = 0.2486	KO: $F_{1,21}$ = 1.714, P = 0.2053	$F_{1,21}$ = 4.565, P = 0.0452
	Bip	Two-way ANOVA	n=6~7	MPTP: $F_{1,21}$ = 8.817, P = 0.0073	KO: $F_{1,21}$ = 0.0281, P = 0.8685	$F_{1,21}$ = 11.84, P = 0.0025
	p-IRE1/IRE1	Two-way ANOVA	n=6~7	MPTP: $F_{1,21}$ = 15.29, P = 0.0008	KO: $F_{1,21}$ = 18.84, P = 0.0003	$F_{1,21}$ = 4.411, P = 0.048
	sXBP-1	Two-way ANOVA	n=6~7	MPTP: $F_{1,21}$ = 5.806, P = 0.0248	TPPU: $F_{1,21}$ = 9.558, P = 0.0053	$F_{1,21}$ = 0.6413, P = 0.4318
	p-JNK/JNK	Two-way ANOVA	n=6~7	MPTP: $F_{1,21}$ = 8.730, P = 0.0073	KO: $F_{1,21}$ = 3.841, P = 0.0628	$F_{1,21}$ = 4.822, P = 0.0389
	ATF6	Two-way ANOVA	n=6~7	MPTP: $F_{1,21}$ = 3.671 P = 0.0679	KO: $F_{1,21}$ = 8.863, P = 0.0067	$F_{1,21}$ = 25.40, P < 0.0001
	cATF6	Two-way ANOVA	n=6~7	MPTP: $F_{1,21}$ = 1.308, P = 0.265	KO: $F_{1,21}$ = 6.227, P = 0.0201	$F_{1,21}$ = 10.92, P = 0.0032
	p-p38/p38	Two-way ANOVA	n=6~7	MPTP: $F_{1,21}$ = 4.274, P = 0.0501	KO: $F_{1,21}$ = 1.095, P = 0.3063	$F_{1,21}$ = 6.248, P = 0.0197
Fig.3 C	iNOS	Two-way ANOVA	n=6~7	MPTP: $F_{1,21}$ = 17.10, P = 0.0005	TPPU: $F_{1,21}$ = 14.08, P = 0.0012	$F_{1,21}$ = 4.644, P = 0.0429
	SOD	Two-way ANOVA	n=6~7	MPTP: $F_{1,21}$ = 5.253, P = 0.0319	TPPU: $F_{1,21}$ = 0.0017, P = 0.9676	$F_{1,21}$ = 12.52, P = 0.0018
Fig.3 D	iNOS	Two-way ANOVA	n=6~7	MPTP: $F_{1,21}$ = 8.234, P = 0.0098	KO: $F_{1,21}$ = 0.008, P = 0.0317	$F_{1,21}$ = 11.57, P = 0.003
	SOD	Two-way ANOVA	n=6~7	MPTP: $F_{1,21}$ = 5.008, P = 0.0347	KO: $F_{1,21}$ = 4.788, P = 0.0414	$F_{1,21}$ = 1.208, P = 0.2854
Fig.5 E	TH-positive cells	Two-way ANOVA	n=4	PARK2: $F_{1,12}$ = 0.3090, P = 0.5885	TPPU: $F_{1,12}$ = 1.866, P = 0.197	$F_{1,12}$ = 0.0032, P = 0.956
Fig.5 F	Cleaved caspase-3	Two-way ANOVA	n=4	PARK2: $F_{1,12}$ = 9.999, P = 0.0082	TPPU: $F_{1,12}$ = 5.356, P = 0.0392	$F_{1,12}$ = 2.467, P = 0.142

Table S2. Levels of eicosanoids metabolites in the striatum.

	Control			MPTP			P value
6-keto-PGF1a	19.967	±	1.629	20.015	±	1.352	0.653
TXB2	103.088	±	8.432	98.406	±	4.740	0.866
9,12,13-TriHOME	69.431	±	18.606	59.487	±	4.168	0.582
9,10,13-TriHOME	40.382	±	10.250	33.635	±	2.452	0.495
PGF2a	**207.788**	**±**	**9.015**	**160.704**	**±**	**7.212**	**0.021**
PGE2	15.900	±	0.477	13.830	±	1.069	0.190
PGD2	149.644	±	8.398	127.452	±	4.968	0.071
15,16-DiHODE	4.004	±	0.542	3.667	±	0.609	0.498
12,13-DiHOME	7.095	±	0.390	8.348	±	1.710	0.714
9,10-DiHOME	**3.226**	**±**	**0.601**	**1.346**	**±**	**0.158**	**0.004**
19,20-DiHDPE	4.092	±	0.792	5.310	±	0.523	0.392
EKODE	19.927	±	6.196	23.007	±	4.170	0.700
13-HODE	47.613	±	11.285	58.399	±	5.240	0.326
9-HODE	40.195	±	6.041	41.360	±	3.045	0.710
15-HETE	124.063	±	11.440	129.113	±	6.703	0.484
11-HETE	123.175	±	9.516	114.056	±	5.188	0.587
9-oxo-ODE	33.256	±	5.598	46.977	±	5.160	0.072
12-HETE	102.788	±	8.210	136.621	±	26.845	0.171
12(13)-EpOME	7.595	±	1.590	7.073	±	0.689	0.745
14(15)-EpETrE	89.347	±	7.351	77.976	±	11.479	0.512
9(10)-EpOME	6.158	±	0.899	6.641	±	0.431	0.607
10(11)-EpDPE	**5.301**	**±**	**1.525**	**9.530**	**±**	**0.829**	**0.015**
11(12)-EpETrE	71.998	±	6.178	61.583	±	4.605	0.235
8(9)-EpETrE	**36.708**	**±**	**4.502**	**19.048**	**±**	**1.310**	**0.001**
5(6)-EpETrE	516.259	±	30.771	544.908	±	19.111	0.447

The values are the mean +/- SEM (n = 6).
Student t-test was used.
The bold was statistical significant.

Table S3. Information of antibodies used in this study

Marker		Species,Isotype	Label	Dilution	Maker	Catalog number
Primary antibody	Phospho-PERK(Thr980)	Rabbit IgG	–	1:1000	Cell Signaling Technology	#3179
	PERK	Rabbit IgG	–	1:1000	Cell Signaling Technology	#3192
	Phospho-eIF2α(Ser51)	Rabbit IgG	–	1:1000	Cell Signaling Technology	#3398
	eIF2α	Rabbit IgG	–	1:1000	Cell Signaling Technology	#5324
	Bip	Rabbit IgG	–	1:1000	Cell Signaling Technology	#3177
	IRE1α(phospho S724)	Rabbit IgG	–	1:1000	abcam	ab38187
	IRE1α	Rabbit IgG	–	1:1000	Cell Signaling Technology	#3294
	XBP-1s	Rabbit IgG	–	1:1000	Cell Signaling Technology	#12782
	JNK1+JNK2(phspho T183+Y185)	Rabbit IgG	–	1:1000	abcam	ab4821
	JNK1+JNK2	Rabbit IgG	–	1μg/ml	abcam	ab112501
	ATF6	Rabbit IgG	–	1:1000	Cell Signaling Technology	#65880
	Phospho-p38 MAPK(Thr180/Tyr182)	Rabbit IgG	–	1:1000	Cell Signaling Technology	#4511
	p38 MAPK	Rabbit IgG	–	1:1000	Cell Signaling Technology	#8690
	Glutathione	Mouse IgG	–	1:1000	abcam	ab19534
	iNOS	Rabbit IgG	–	1:500	abcam	ab3523
	Superoxide Dismutase1	Rabbit IgG	–	0.2μg/ml	abcam	ab13498
	Tyrosine Hydroxylase	Rabbit IgG	–	1:1000	Merck Millipore	AB152
	DAT	Rat IgG	–	1:10000 or 1:1000	Merck Millipore	MAB369
	OX42	Rat IgG	–	1μg/ml	abcam	ab1211
	α-Synuclein (phospho S129)	Rabbit IgG	–	1:5000	abcam	ab51253
	α-Synuclein	Mouse IgG	–	1:500	BD Transduction Laboratories	610787
	mouse sEH	Rabbit IgG	–	1:5000	UC Davis	–
	Human sEH	Rabbit IgG	–	1:10000	UC Davis	–
	β-Actin	Mouse IgG	–	1:10000	Sigma-Aldrich	A5441
	β3-tubulin	Mouse IgG2b	–	1:1000	Sigma-Aldrich	T8660
	Tyrosine Hydroxylase	Mouse IgG1	–	1:500	Sigma-Aldrich	T1299
	Cleaved Caspase-3	Rabbit IgG	–	1:400	Cell Signaling Technology	#9661
Secondary antibody	Anti-rabbit IgG	Goat IgG	–	1:10000	GE healthcore	NA934
	Anti-mouse IgG	Goat IgG	–	1:10000	GE healthcore	NA931
	Anti-Rat IgG	Goat IgG	–	1:10000	GE healthcore	NA935
	Anti-rabbit IgG	Goat IgG	Alexa Fluor 488	1:1000	Invitrogen	A11070
	Anti-mouse IgG2b	Goat IgG	Alexa Fluor 647	1:500	Invitrogen	A21242
	Anti-mouse IgG1	Goat IgG	Alexa Fluor 488	1:500	Invitrogen	A21121
	Anti-rabbit IgG	Goat IgG	Alexa Fluor 555	1:500	Invitrogen	A21429
	Anti-Rat IgG	Goat IgG	Alexa Fluor 647	1:1000	Invitrogen	A21247
Other	bisBenzimide H 33258 (Hoechst)				Tokyo Chemical Industry Co., Ltd.	H1343